APPENDIX A

Transfer of P-type to N-type Thermoelectric Properties of Ag-Sb-Te Thin Film Temperature Annealing and Its Electrical Power Generation

Journal of ELECTRONIC MATERIALS
https://doi.org/10.1007/s11664-019-07756-9

Transfer of *P*-type to *N*-type Thermoelectric Properties of Ag-Sb-Te Thin Film Through Temperature Annealing and Its Electrical Power Generation

NATCHANUN PRAINETR,[1] ATHORN VORA-UD,[1,2,3,7] MATI HORPRATHUM,[4] PENNAPA MUTHITAMONGKOL,[5] SOMPORN THAOWONKAEW,[1,2] THEERAPONG SANTHAVEESUK,[1] THANG BACH PHAN,[6] and TOSAWAT SEETAWAN[1,2,3,8]

1.—Program of Physics, Faculty of Science and Technology, Sakon Nakhon Rajabhat University, 680 Nittayo Road, Mueang District, Sakon Nakhon 47000, Thailand. 2.—Thin Films Laboratory, Center of Excellence for Alternative Energy, Research and Development Institution, Sakon Nakhon Rajabhat University, 680 Nittayo Road, Mueang District, Sakon Nakhon 47000, Thailand. 3.—Thailand Center of Excellence in Physics, Ministry of Higher Education, Science, Research and Innovation, 328 Si Ayutthaya Road, Bangkok 10400, Thailand. 4.—National Electronics and Computer Technology Center, 114 Thailand Science Park, Paholyothin Rd., Klong 1, Klong Luang, Pathumthani 12120, Thailand. 5.—National Metal and Materials Technology Center, National Science and Technology Development Agency, Klong Luang, Pathumthani 12120, Thailand. 6.—Center for Innovation Materials and Architectures (INOMAR) and Laboratory of Advanced Materials, University of Science, Vietnam National University, Ho Chi Minh City, Vietnam. 7.—e-mail: athornvora-ud@snru.ac.th. 8.—e-mail: t_seetawan@snru.ac.th

Ag-Sb-Te (AST) thin film was successfully fabricated on a flexible polyimide substrate by using DC magnetron sputtering from the AgSbTe (AST) target. As-deposited samples were annealed at temperatures between 300 and 450°C under vacuum for 30 min. Then, uni-leg AST thin film thermoelectric modules of five elements were fabricated. Thermal annealing induced a change of thermoelectric characteristic of the thin film from *p*-type material (300–350°C) to *n*-type material (400–450°C) through the change in structures (amorphous to crystalline, atomic composition ratio and surface roughness, etc.). The highest power factor was 0.97 mW m^{-1} K^{-2} and 0.065 mW m^{-1} K^{-2} for *p*-type and *n*-type, respectively. The maximum power generation of the uni-leg AST thin film thermoelectric module was approximately 0.88 nW for *p*-type and 0.54 nW for *n*-type, with a temperature difference of around 20 K.

Key words: Flexible thin film thermoelectric, Ag-Sb-Te thin films, DC magnetron sputtering

INTRODUCTION

Nowadays, the requirement of energy is very important and trending to employ fuel energy, such as oil, natural gas, and coal, and it has been increasing. The development of renewable energy is interesting to researchers and innovation works. Thermoelectricity (TE) is an energy technology of interest which can be applied to renewable energy.[1–3] TE generation has primarily been directed toward increasing the material figure of merit (ZT), defined as, $ZT = \frac{S^2 T}{\rho \kappa}$, where S is the Seebeck coefficient, ρ is the electrical resistivity, and κ is the total thermal conductivity, and T is the absolute temperature. The S^2/ρ term is called the thermoelectric power factor (PF).[4] However, PF value is requested of maximum to be affected by high electrical power of TE module. In this case, we

(Received August 10, 2019; accepted October 19, 2019)

Journal : 11664_JEM | Dispatch : 29-10-2019 | Pages : 6
Article No.: 7756 | ☐ LE ☑ CP | ☐ TYPESET ☑ DISK

suggested an Ag-Sb-Te material because it has received much more attention for the thermoelectric devices with high ZT (around 1.55 at 533 K).[5] This material is called a chalcogenide alloy, with application in phase-change memory devices[6–8] and thermoelectric (TE) technologies.[9–12] This material has a cubic rock-salt structure (Fm-3m) in which Na sites are occupied by Ag or Sb randomly.[11] Hence, the Ag/Sb ratio is disordered atomic to modulate the narrow band gap energy or display semimetal behaviors[13–15] which are very important for thermoelectric properties.[11] For AST bulk material at room temperature, the authors reported high power factor around 153–2340 $\mu W\ m^{-1}\ K^{-2}$ and low thermal conductivity around 0.3–0.7 $Wm^{-1}\ K^{-1}$.[16–19] In the case of a thermoelectric generator, the flexible thin film thermoelectric is of extensive interest for use in the microscale industry and wearable electronics.[20] In addition, the ZT value can be improved due to the decrease in thermal conductivity with phonon scattering in thin film materials.[20,21]

In this work, we fabricated the uni-leg AST thin film thermoelectric module with five elements on a flexible polyimide substrate by using DC magnetron sputtering. Crystal structure, microstructural, composition and thermoelectric properties of the AST films were controlled by the annealing temperature (300 to 450°C). Then, the power generation of the module was also investigated.

EXPERIMENTAL DETAILS

AST thin films are deposited on polyimide flexible substrates by DC magnetron from an AgSbTe (1:1:1 ratio) target of 99.99% purity (ULVAC Technologies, Inc.) which are 59.0 mm in diameter and 3.0 mm in thickness. Before deposition, the base pressure for the high vacuum was required to be under 4.0×10^{-3} Pa. The depositing pressure is about 2.67 Pa with the Ar gas flow rate of 30 sccm. DC power supply for film deposition is 40 W and the film thickness is around 100-150 nm. After deposition, the as-deposited thin films were annealed at a high temperature range (300°C to 500°C) under a high-vacuum furnace (Lenton) for 30 min. Phase identification of AST thin films was analyzed using x-ray diffraction (XRD6100, Shimadzu) with a Cu source (λ = 1.54 Å) as used 40 kV and 40 mA in conventional $\theta - 2\theta$ mode from 20° to 55° at a step of 0.02° and a scanning rate of 8°/min. The atomic composition was examined using energy dispersive x-ray spectroscopy (EDX) (SU8030, Hitachi). The surface morphologies and roughness were examined using atomic force microscopy (XE-120, Park Systems) in force modulation mode. The Hall Effect was measured at room temperature under 0.55 T with a four-probe configuration using the Van der Pauw method (HMS-3000, Ecopia). The thermoelectric properties, Seebeck coefficient and electrical resistivity, were measured using a ZEM-3 instrument (ZEM-3, Advance Riko).

The annealed thin films were used to fabricate a flexible uni-leg thin film module with five pairs on a polyimide substrate as shown in Fig. 1a and b. Five TE elements of 2.0 mm × 20 mm were configured in-plane with the polyimide substrate (25.40 mm^2 × 25.40 mm^2) area, Silver (Ag) was used to make electrode series between TE elements. Figure 1c and d displayed the model and real image of our TE

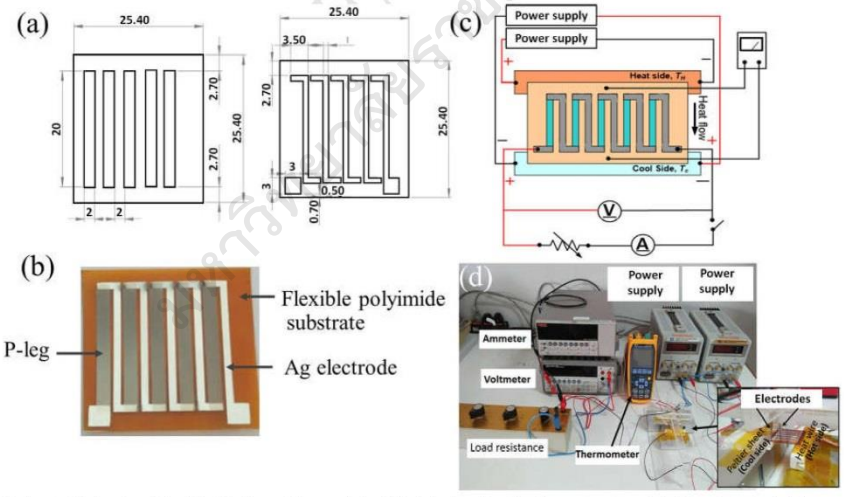

Fig. 1. (a) design to fabrication of flexible thin film uni-leg module, (b) fabrication five TE elements onto polyimide substrate, (c) the model and (d) real image of TE generation measurement system.

Journal : 11664_JEM | Dispatch : 29-10-2019 | Pages : 6
Article No.: 7756 | ☐ LE ☑ CP | ☐ TYPESET ☑ DISK

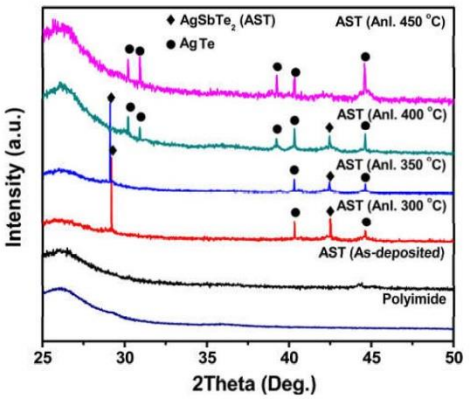

Fig. 2. XRD patterns of AST thin films on polyimide flexible substrates as annealed at different temperature.

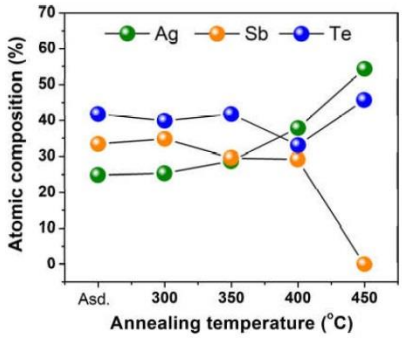

Fig. 3. The atomic composition of AST thin film with various annealing temperatures.

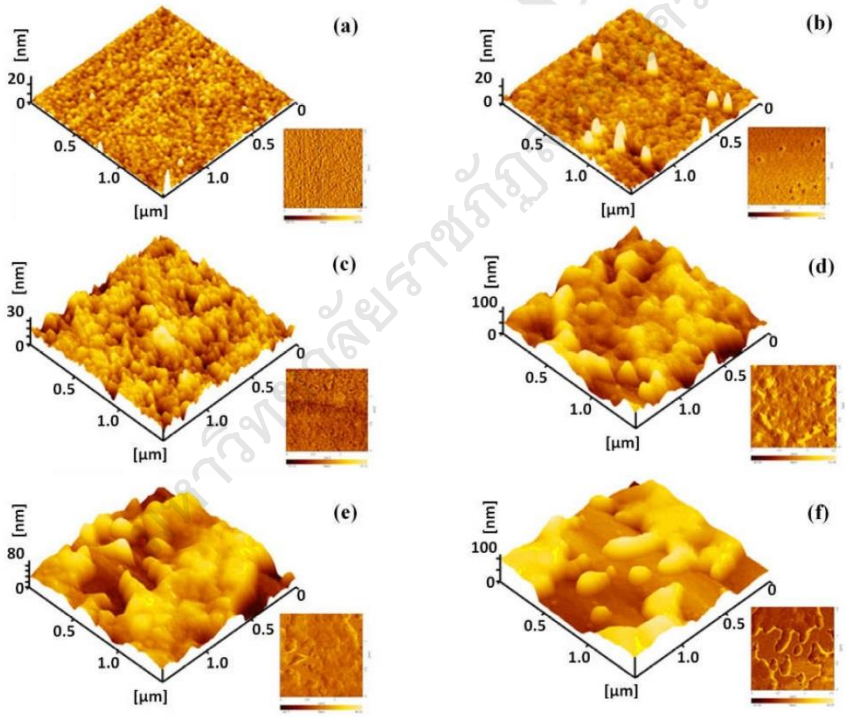

Fig. 4. AFM 3D images of AST thin film surface morphology and roughness with various annealing temperatures: (a) As-deposited, (b) 300°C, (c) 350°C, (c) 400°C and (e) 450°C.

Journal : 11664_JEM | Dispatch : 29-10-2019 | Pages : 6
Article No.: 7756 | ☐ LE ☑ CP | ☐ TYPESET ☑ DISK

generator measurement system. The open voltage (V_o) was measured using a six-digit multimeter (M3500A, Picotest) at difference temperatures (ΔT). At ΔT with highest V_o, the ΔT was soaked to measure the electrical current (I) using a picoammeter (648 pm, Keithley) and output voltage (V) within the various of load resistance (R_L) applied until 10 MΩ to calculate the electrical power ($P = VI$).

RESULTS AND DISCUSSION

The XRD patterns of AST films were shown in Fig. 2. These results showed that the as-deposited thin film tended to be amorphous and then became crystalline as mixed between AgTe and $AgSbTe_2$ phases after thermal annealing. The major diffraction peak of AgTe (PDF#1600412) appeared at 2θ = 30.94°, 31.39°, 38.82°, 40.45° and 45.11°, corresponding to (231), (320), (261), (090) and (222) planes, respectively. Meanwhile, $AgSbTe_2$ (PDF#893671) occurred at 2θ = 29.37° and 42.52°, corresponding to (200) and (220) planes. It is noted that the thin film annealed up to 400°C slowly decomposed to an AgTe phase and then completed to an AgTe single phase at higher annealing temperature (450°C). The intensity of AgTe phases was gradually enhanced as the annealing temperature increased due to the evaporation of antimony at a high annealing temperature.[22] The effect of annealing temperature on the chemical composition of thin film was studied using EDX, as displayed in Fig. 3. Ag and Te suddenly increased as annealing temperature increased to 450°C close to the melting point Sb. 3D AFM images of the as-deposited and annealed AST films are presented in Fig. 4. The analysis result of these sample images showed that the roughness increased with temperature annealing, approximately 0.69 nm for as-deposited films, and 1.35 nm, 2.82 nm, 15.09 nm and 16.08 nm for the annealed films at 300°C, 350°C, 400°C and 450°C, respectively. From Fig. 4a, surface morphology of the as-deposited amorphous thin film shows smooth roughness and high homogeneity, while the surface of annealed samples (Fig. 4b–d) showed a gradual island-like shape and sharp spike which may be the result of oriented grains pushing out of the thin film during annealing at high temperature (300°C to 400°C). Moreover, the surface of the thin film annealed at 450°C containing a main AgTe phase (Fig. 4e) displayed a dramatic change due to the evaporation of antimony. This is because the bonding energy of the Ag-Te bond is a less than the Sb-Te bond of around 81.60 kJ mol^{-1}.[23] These results indicate that the high-temperature annealing has influenced the phase transformation in AST thin film ($AgSbTe_2$ and AgTe mix phases to AgTe pure phase) and possibly affects the thermoelectric properties of thin film which will be discussed in the next section.

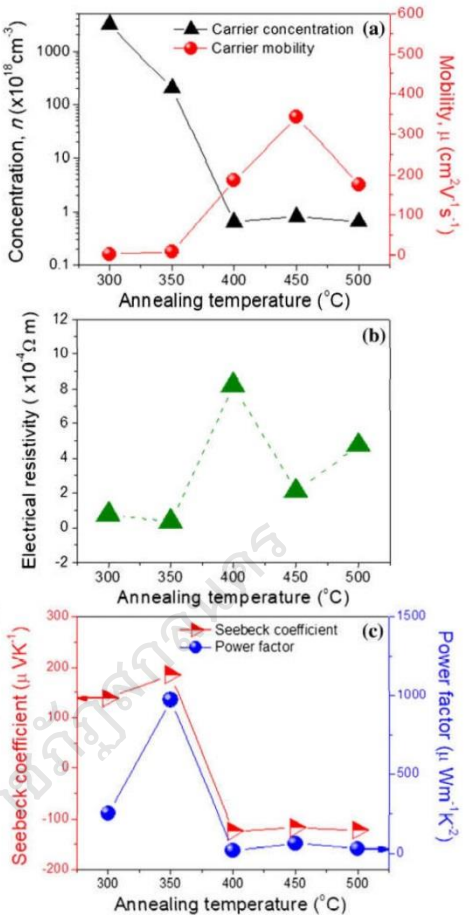

Fig. 5. Thermoelectric properties of AST thin films (a) carrier concentration and mobility, (b) electrical resistivity and (c) Seebeck coefficient and power factor as annealing temperature functions.

The carrier concentration and mobility method of the AST thin film obtained using the Hall effect are presented in Fig. 5a. The carrier concentration decreased gradually and the mobility increased with increasing annealing temperature. Those dependencies might come from acoustic phonon scattering in the sample due to increasing content of an Ag-Te phase[18] and also the charge discrepancy of non-stoichiometric ratios between Ag and Te.[11] The electrical resistivity of the AST thin film was determined from concentration and mobility values[4] as follows: $\rho = \frac{1}{n|\mu q}$, where q is carrier charge, n is carrier concentration, and μ is carrier mobility. Figure 5b shows the electrical resistivity of the

Journal : 11664_JEM | Dispatch : 29-10-2019 | Pages : 6
Article No.: 7756 | ☐ LE ☑ CP | ☐ TYPESET ☑ DISK

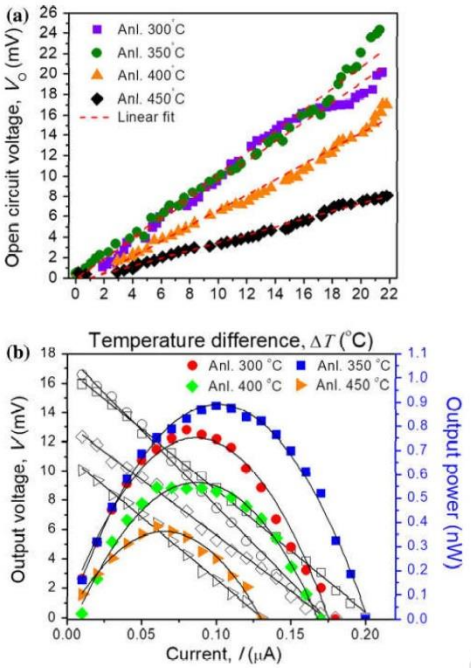

Fig. 6. (a) The V_o of TE thin film modules within the ΔT increasing and (b) P_{max} values (color scatters) versus output voltage (open scatters) as same the scatter type and electrical current.

annealed sample, which tended to increase with the annealing temperature. At an annealing temperature of 350°C, the thin film has a minimum resistivity ρ of 0.35×10^{-4} Ω m. Figure 5c shows the Seebeck coefficient and power factor of the AST thin film as various annealing temperatures. It is noted that the annealing temperature changed the thermoelectric properties of thin film from *p*-type material (300–350°C) to *n*-type material (400–450°C) due to structural change as mentioned above. Moreover, these results claim that the *p*-type and *n*-type of AgTe depend on the composition of the Ag:Te ratio, and the Ag-Te was *n*-type because there was more Ag than Te in the ratio[24] as corresponds to the film annealed at 400 and 450°C. Moreover, the narrow band gap semiconductor behavior of these materials unbalanced the number of electrons and holes in a two-carrier system.[15,25] The power factor ($PF = S^2/\rho$) is an important thermoelectric parameter which is calculated by relative the Seebeck coefficient and electrical resistivity. The power factor as calculated follows the Seebeck coefficient increases first and then decreases suddenly with high electrical resistivity and low Seebeck coefficient at annealing temperatures of 400°C and 450°C. The maximum Seebeck coefficient and power factor of 186 $\mu V\ K^{-1}$ and 0.97 $mW\ m^{-1}\ K^{-2}$, respectively, were obtained from the film annealed at 350°C.

In case of power generation, the V_O of thin film modules were linearly increased with the increase of ΔT, as shown in Fig. 6a. The maximum output power P_{max} values versus output voltage and current as illustrated in Fig. 6b. At ΔT = 20°C (hot side of 50°C and cool side of 30°C), the TE module with thin film annealed at 350°C had shown the highest open voltage approximately 22 mV and the maximum power around 0.90 nW with the R_L at 1 MΩ.

CONCLUSION

The AST thin films were successfully deposited on the polyimide substrate using DC magnetron sputtering. The annealing temperature has an effect on microstructure, morphology, composition and thermoelectric properties of AST thin films. The as-deposited thin films showed an amorphous phase and then became mixed crystalline of Ag_2Te and Sb_2Te_3 phases after annealing. The film annealed at 350°C showed good TE properties with the maximum Seebeck coefficient and power factor around 186 $\mu V\ K^{-1}$ and 0.97 $mW\ m^{-1}\ K^{-2}$, respectively. Moreover, its TE module could generate a maximum power of approximately 0.90 nW (at ΔT = 20°C).

ACKNOWLEDGMENTS

This work was financially supported by the National Research Council of Thailand (NRCT) and Thailand Research Fund (TRF) through Research Career Development Grant (RSA6180070) and the TRF-MRG Young Scientific Researcher (Grant No. MRG6180007).

REFERENCES

1. R. Venkatasubramanian, E. Siivola, T. Colpitts, and B. Quinn, *Nature* 413, 597 (2001).
2. R. Ahısk and H. Mamur, *Int. J. Renew. Energ. Res.* 4, 128 (2014).
3. A. Weidenkaff, *EPJ Web of Conferences*, vol. 148 (2017), p. 00010.
4. A. Vora-ud, M. Horprathum, M. Kumar, P. Muthitamongkol, C. Chananonnwathorn, B. Saekow, I. Nualkham, S. Thaowonkaew, C. Thanachayanont, and T. Seetawan, *Mater. Lett.* 234, 229 (2019).
5. J.J. Xu, H. Li, B.L. Du, X.F. Tang, Q.J. Zhang, and C. Uher, *J. Mater. Chem.* 20, 6138 (2010).
6. T. Ohta, K. Nishiuchi, K. Narumi, Y. Kitaoka, H. Ishibashi, N. Yamada, and T. Kozaki, *Jpn. J. Appl. Phys.* 39, 770 (2000).
7. T. Maeda, M. Terao, and T. Shimano, *Jpn. J. Appl. Phys.* 42, 1044 (2003).
8. J. Xu, B. Liu, Z. Song, S. Feng, and B. Chen, *Mater. Sci. Eng. B* 127, 228 (2006).
9. B. Du, H. Li, J. Xu, X. Tang, and C. Uher, *Chem. Mater.* 22, 5521 (2010).
10. J. Zhang, X. Qin, D. Li, C. Song, Y. Liu, H. Xin, T. Zou, and Y. Li, *Electron. Mater. Lett.* 11, 133 (2015).
11. J. Kim, J.Y. Lee, J.H. Lim, and N.V. Myung, *Electrochim. Acta* 196, 579 (2016).
12. M. Salimi and S. Javad Hashemifar, *J. Alloys Compd.* 650, 143 (2015).
13. L.-H. Ye, K. Hoang, A.J. Freeman, S.D. Mahanti, J. He, T.M. Tritt, and M.G. Kanatzidis, *Phys. Rev. B* 77, 245203 (2008).

Journal : 11664_JEM | Dispatch : 29-10-2019 | Pages : 6
Article No.: 7756 | ☐ LE ☑ CP | ☐ TYPESET ☑ DISK

14. K. Wojciechowski, J. Tobola, M. Schmidt, and R. Zybala, *J. Phys. Chem. Solids* 69, 2748 (2008).
15. V. Jovovic and J. Heremans, *Phys. Rev. B* 77, 245204 (2008).
16. H. Ma, T. Su, P. Zhu, J. Guo, and X. Jia, *J. Alloys Compd.* 454, 415 (2008).
17. H. Wang, J.-F. Li, M. Zou, and T. Sui, *Appl. Phys. Lett.* 93, 202106 (2008).
18. S.N. Zhang, T.J. Zhu, S.H. Yang, C. Yu, and X.B. Zhao, *J. Alloys Compd.* 499, 215 (2010).
19. J. Xu, H. Li, B. Du, X. Tang, Q. Zhang, and C. Uher, *J. Mater. Chem.* 20, 6138 (2010).
20. Z.H. Zheng, J.T. Luo, T.B. Chen, X.H. Zhang, G.X. Liang, and P. Fan, *Appl. Phys. Lett.* 112, 163901 (2018).
21. P. Wanarattikan, P. Jitthammapirom, R. Sakdanuphab, and A. Sakulkalavek, *Adv. Mater. Sci. Eng.* 2019, 6954918 (2019).
22. A. Vora-ud, M. Horprathum, M. Kumar, P. Muthitamongkol, C. Chananonnawathorn, B. Saekow, I. Nualkham, S. Thaowonkaew, C. Thanachayanont, and T. Seetawan, *Mater. Lett.* 234, 229 (2019).
23. Y.R. Luo, *Comprehensive Handbook of Chemical Bond Energies* (Boca Raton: CRC Press, 2007).
24. U. Shinde, *Adv. Appl. Sci. Res.* 8, 55 (2017).
25. D. Morelli, V. Jovovic, and J. Heremans, *Phys. Rev. Lett.* 101, 035901 (2008).

Journal : 11664_JEM | Dispatch : 29-10-2019 | Pages : 6
Article No.: 7756 | ☐ LE ☑ CP | ☐ TYPESET ☑ DISK